Flow Prediction around a NACA0012 Airfoil at low Reynolds Number

A Project Report Submitted by

Subham Kant Das

Contents

List of Figures

Chapter 1

Introduction

Since the past few decades, there has been an increased interest in the field of Micro Aerial Vehicles(MAVs) and their potential application in the defense sector. Their reduced size, coupled with higher payload capacity, has extended their use to various other sectors. However, due to the smaller size followed by shorter wingspan, the chord-based Reynolds Number for MAV is very less(of the order of 1000), which leads to poor performance in the range of operation. Hence to improve their performance, it becomes essential to study the flow characteristics at such low Reynolds Number. The flow in this regime consists of complex phenomena such as the transition from laminar to the turbulent regime, flow separation, and reattachment followed by the formation of laminar separation bubble. Although the flow is initially laminar, the entire phenomenon cannot be captured using conventional laminar models. Thus the flow around airfoils at low Reynolds Number is intriguing to researchers.

One of the pioneering works to understand the transition in performance of airfoils was performed by McMasters and Henderson. According to their study,

Figure 1.1: RQ-16 T-Hawk MAV Designed and Developed by Honeywell, Source: navy.mil
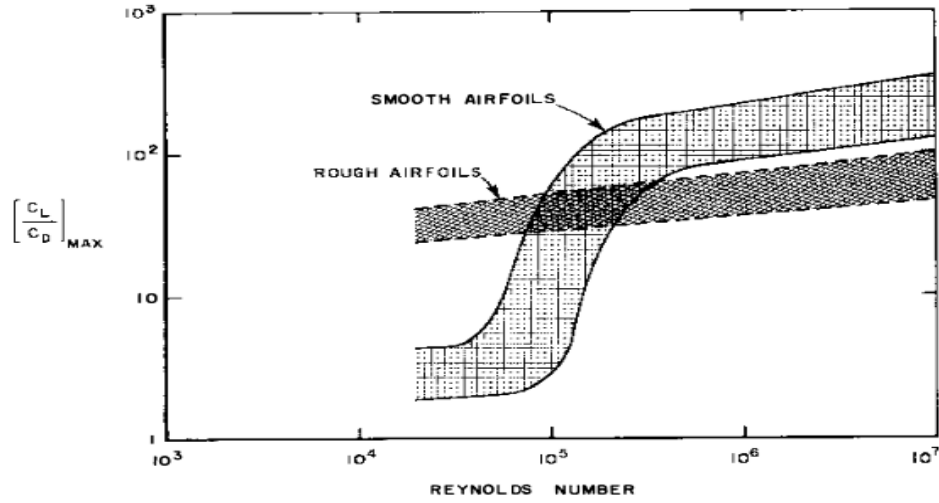
Figure 1.2: Performance of Rough and Smooth Airfoils at different Reynolds Number, Source: Henderson et. al[4]

airfoils fail to show appreciable performance(measured by the ratio of lift to drag coefficient) at a Reynolds Number of 70000, which was estimated to be the critical Reynolds Number. The performance of the airfoil starts to improve with Reynolds Number as we move beyond the critical Reynolds Number. However, since MAVs operate on ultralow Reynolds Number which is less than the critical Reynolds Number identified by McMasters and Henderson, although the flow is laminar in this regime, it is governed by complex phenomena such as flow separation, vortex shedding, formation of laminar separation bubble and reattachment. As the angle of attack is increased, these behaviour become even more difficult to capture using conventional numerical models.

1.1 Motivation

It is relatively easier to predict the flow behaviour at the higher Reynolds Number using conventional models since the flow remains attached to the surface of the airfoil, or the separation, if happens, is delayed. However at ultralow Reynolds Number(here 1000) where the flow should be characterized as laminar, conventional models fail to capture the physics. The reason for this is the fluid particle not having enough energy to sustain the adverse pressure gradient, leading to flow separation. As the flow separates, transition from laminar to turbulent regime takes place and the fluid particle gains energy, thereby reattaching to the surface, forming a separation bubble. Thus the flow actually is neither fully laminar nor fully turbulent, but rather a blend of both with a transition region in between.

Higher the angle of attack, higher the complexity in the flow. LES and DNS can yield promising results, however they are memory intensive and require significant computing power. In an attempt to improve the performance of MAVs without the need of memory intensive computations, it becomes necessary to evaluate the performance of 2D RANS model and identify the regions where improvements are to be made.

1.2 Problem Statement

The objective of this study is to numerically examine the effect of solver flow type(laminar or turbulent), meshing resolution and domain extent on the flow physics around a NACA0012 Airfoil at low Reynolds Number(1000). The rectangular domain shown in Figure 1(a) is used for the present study since the mesh can be easily controlled near the Trailing Edge to capture the wake. The present work will evaluate the ability of the laminar and Spalart Allmaras(SA) model to predict the flow behavior at a Reynolds Number of 1000 using the PISO algorithm in OpenFOAM. The effect of domain extent and mesh resolution will be studied, and the results will be validated against available literature.

Chapter 2

Literature Review

2.1 Theory

2.1.1 Concept of Lift and Drag

When it comes to external aerodynamics, lift and drag are the most important factors to consider. During mechanical interaction between two solid bodies, forces are developed at the point of contact. Since solids are rigid, the forces can be computed with a relative ease. But since fluids are prone to change shape, the forces developed are difficult to describe. Here, the point of contact is the wetted surface of the solid-liquid interface. Things become more complicated when fluids starts to separate from the surface under the influence of an adverse pressure gradient. The forces that acts on the solid is perpendicular to its surface. It can, thus be resolved into two different components, one along the flow direction and the other perpendicular to it. The component of the force which is along the flow direction is called the drag force while the component perpendicular to the surface is the lift force. The lift force is desirable in order to increase the elevation whereas the drag force acts as a parasite, and is responsible for excess fuel consumption. In order to take the scaling effect into account two dimensionless parameters known as Drag and Lift coefficients are defined as:

$$C_d = \frac{F_D}{\frac{1}{2}\rho A_s U_\infty^2} \quad , \text{and} \quad C_L = \frac{F_L}{\frac{1}{2}\rho A_s U_\infty^2}$$

where,
C_D is the drag coefficient
C_L is the lift coefficient
F_D is the drag force
F_L is the lift force
ρ is the density of the fluid medium

A_s is the spanwise area of the airfoil
U_∞ is the freestream velocity

2.1.2   Computational Domain

In order to study the flow around an airfoil, various types of computational domains are used, rectangular, C, and O domains being the most popular ones. For the purpose of the present study a rectangular domain(Figure 2.1) was used since since the mesh can be easily controlled near the Trailing Edge to capture the wake.
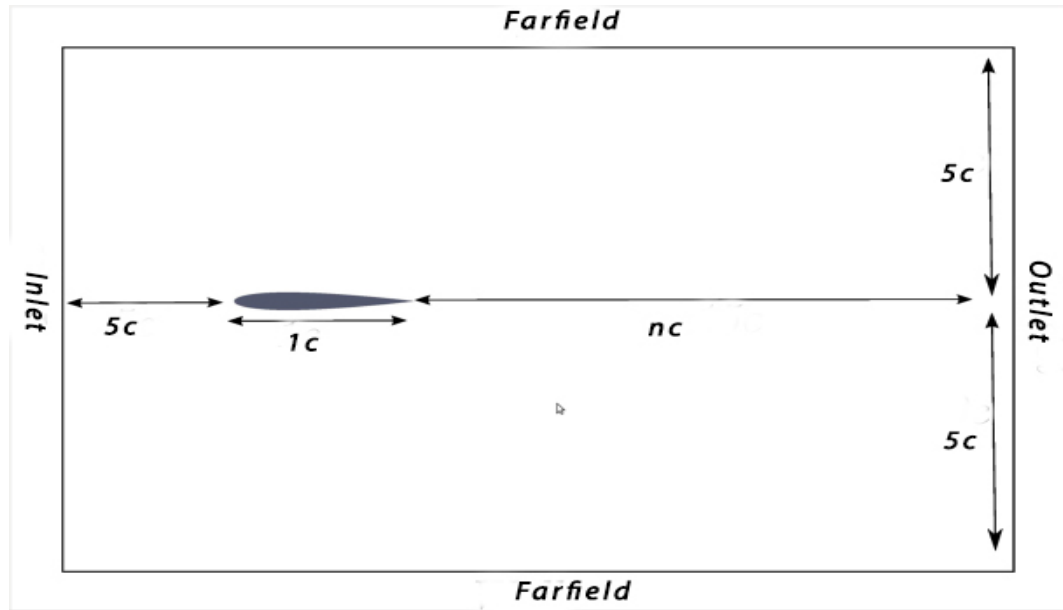
Figure 2.1: A sketch of the rectangular domain used to study flow around NACA0012 airfoil

2.1.3   Turbulence Model

In CFD, RANS(Reynolds Averaged Navier Stokes) is the most widely used turbulence modelling approach. In this approach, the Navier Stokes equations is modified by dividing the velocity into mean and fluctuating components. The total velocity u_i is a function of the mean velocity $\overline{u}$ and the fluctuating velocity u' as shown in the equation below:

$$u_i = \overline{u} + u'$$

As a result of this transformation, a new variable μ_t or turbulent viscosity is introduced into the Navier Stokes equation. The effective viscosity is then given by:

$$\mu_{eff} = \mu_l + \mu_t$$

There are several turbulence models available which solve for μ_t, the number of equation ranges from one to many depending on the model. For the purpose of the present study, the Spalart Allmaras model was used which is a one-equation model solving the modelled transport equation for the kinematic eddy turbulent viscosity. It solves a transport equation for a viscosity-like variable $\tilde{\nu}$ known as the Spalart–Allmaras variable. The turbulent viscosity is then obtained using the following equation:

$$\nu_t = \tilde{\nu} f_{v1}$$

where, f_{v1} is the viscous damping function

2.2 Geometry and Meshing

2.2.1 Equation of NACA0012 Airfoil

A NACA0012 airfoil has zero camber and a maximum thickness of 0.15 times its chord length. As discussed in section 1.1, equation of the NACA0012 is given by:

$$y_t = 0.6[0.2969\sqrt{x} - 0.1260x - 0.3516x^2 + 0.2843x^3 - 0.1015x^5]$$

The mesh was generated using the blockMeshDict utility available in Open-FOAM, since the code can be modified easily in order to yield the desired value of meshing parameters. The different parameters consisting the mesh are the vertices, edges and patches which can be easily seen in Figure 2.3.

Figure 2.2: Vertices, Edges, Blocks and patches in the rectangular domain used to create mesh

2.3   Boundary Conditions
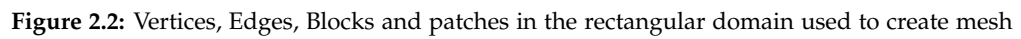
The velocity to be given at the inlet can be determined by the Reynolds Number which is given by,

$$Re = \frac{\rho vc}{\mu} = \frac{\rho vc}{\nu}$$

The Reynolds number for the present study was 1000 and the inlet velocity was calculated accordingly.

constant	values
v	0.1 m/s
ρ	1 g/cm^3
c	1m
ν	1e-03m^2/s

Table 2.1: Values of constants

The inlet gauge pressure was taken to be zero and for determining the values of turbulence modelling parameters, a turbulence intensity(I) of 5% and a turbulent mixing length(l) of 0.25c was taken.
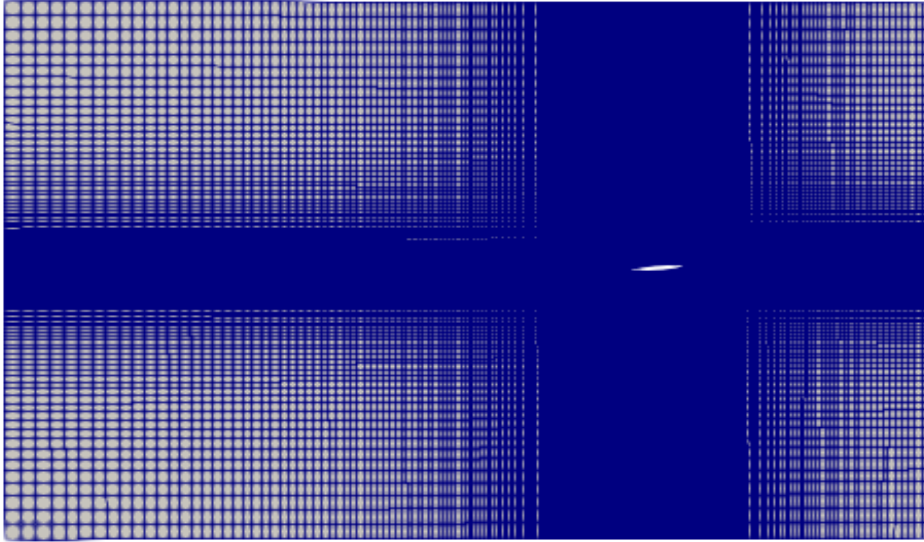
Figure 2.3: Structured Mesh generated using blockMeshDict utility in OpenFOAM

Parameter	Inlet	Outlet	Top and Bottom	Airfoil
u	fixedValue	zeroGradient	fixedValue	noSlip
p	fixedValue	zeroGradient	fixedValue	zeroGradient
$nut, nutilda$	fixedValue	zeroGradient	fixedValue	nutUSpaldingWallFunction
k	fixedValue	zeroGradient	fixedValue	kqRWallfunction
$omega$	fixedValue	zeroGradient	fixedValue	omegaWallfunction

Table 2.2: Boundary Conditions
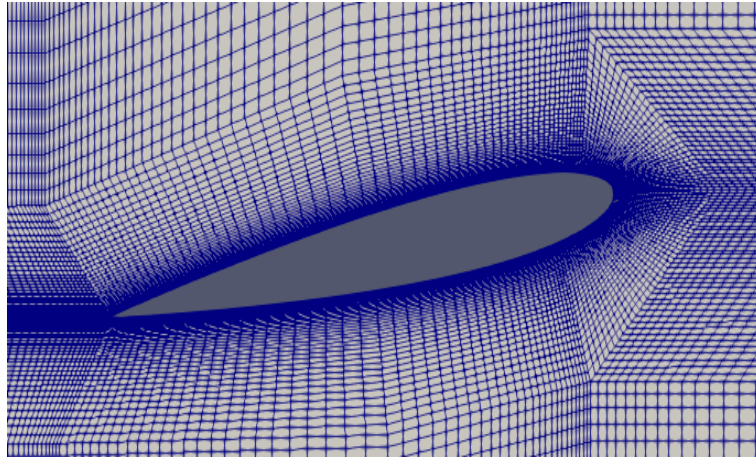
Figure 2.4: Refined grids near the airfoil to capture the flow near the wall

Chapter 3

Effect of Meshing on Airfoil Characteristics

In this section, the effect of domain extension and mesh resolution on flow physics are studied. The data of Liu. et. al. are used to validate the results obtained.

3.1 Nearest Cell Size

YPlus is a a very important parameter to be considered in case of turbulence modelling. It is a measure of the distance of the first cell height from the surface of the wall and is given by(For Reference see [16]):

$$y+ = \frac{U_f \Delta y}{\nu}$$

Where U_f is the friction velocity, and y is the height of the nearest cell to the wall andν is the kinematic viscosity. To ensure that the average yPlus is less than 1 around the airfoil, the CFD solution was run using an arbitrary first cell height. The yPlus was then calculated using the postprocessing utitity "pisoFoam -postProcess -func yPlus -latestTime". Suppose the output gave an average yPlus of x. The first cell height was them reduced by a factor of x to ensure that the average yPlus is less than one around the airfoil.

3.2 Numerical Stability- Courant Number

The Courant number is one of the most important parameters involved in the convergence of a solution. It is determined by the equation:

$$Co = u\frac{\Delta t}{\Delta x} \tag{3.1}$$

where u is the velocity of the fluid particle, Δx is the grid spacing, and Δt is the time step. A Courant number less than one implies that the fluid particle is moving from one grid cell to another in one time step while a courant number greater than one means that the fluid particle is moving through two or more cells in one time step leading to an unstable solution. In order to maintain numerical stability, the courant number was monitored and the time step was adjusted such that the courant number does not exceed 1.

3.3   Effects of Domain Extension

In order to ensure proper convergence of the CFD Solution and to capture the wake, the length of the domain beyond the trailing edge of the airfoil should be large enough. This length is often limited by the computing power available. Here, two different computational domains were taken into consideration.The length of the domain beyond the trailing edge of the airfoil was taken as 10c and 15c respectively ass shown in Figure 3.1. The results obtained was then compared with the experiments of Liu et. al at a Reynolds Number of 1000 and an angle of attack of 5 degrees. The table shows the effect of increasing the domain size on the lift and drag characteristics of the airfoil.

Size of Domain	Angle of Attack	$C_L Num$	$C_L Expt$	Percent Error	$C_D Num$	$C_D Expt$	Percent Error
laminar							
10c	5°	0.2342	0.24	2.41	0.1279	0.128	0.07
15c	5°	0.2342	0.24	2.41	0.1279	0.128	0.07
Spalarat Allmaras							
10c	5°	0.244	0.24	2.08	0.1286	0.128	2.427
15c	5°	0.244	0.24	2.08	0.1286	0.128	2.427

Table 3.1: Comparison of numerical results with the experimental data at Re=1000

From Table 3.1, it can easily be observed that the effect of domain extent on numerical results is negligible and the results obtained are domain independent. The velocity contours for both the domains are shown in Figure 3.2. It can be seen that the flow beyond the trailing edge of of the airfoil is dissipated more effectively in case of a larger domain extent. However since the smaller domain provided reliable results as well, it was taken into consideration for further study.
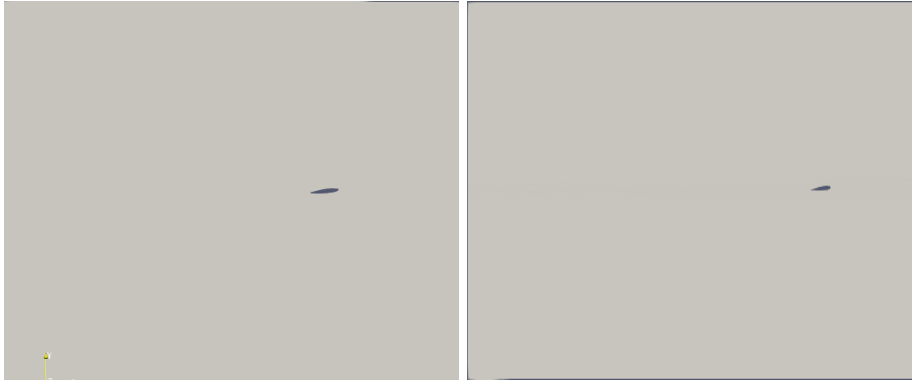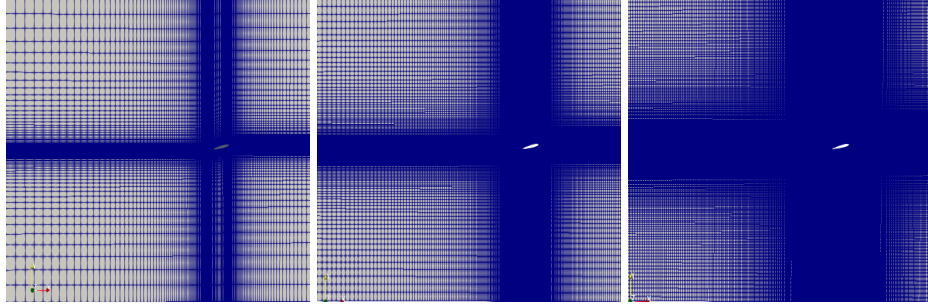
Figure 3.1: Computational domain with domain extent of (a)10c and (b)15c
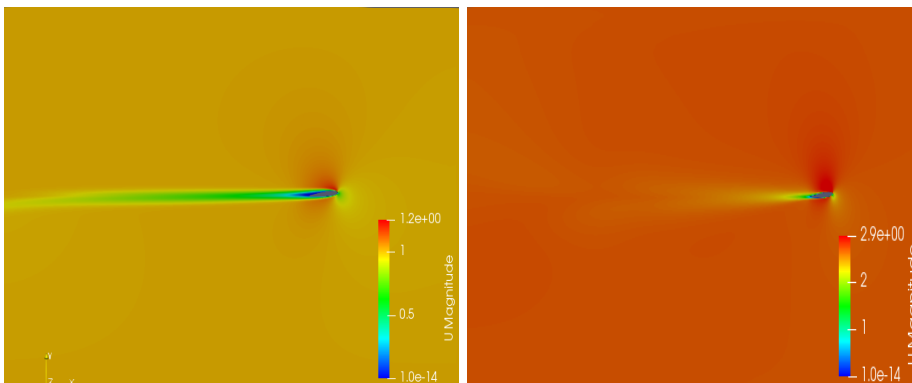
Figure 3.2: velocity contour obtained from the grid for a domain extent of (a)10c and (b)15c at an AoA of 5 degrees

3.4   Grid Independence

Figure 3.3: Grids containing 27150, 108600, and 434400 cells respectively

For the purpose of the present study, a grid refinement study was performed with grids having 27150, 108600, and 434400 cells respectively. The data used for validation was that of Liu et. al. at a Reynolds number of 1000 and an angle of attack of 5 degrees. The coarser grid over-predicted the lift coefficient and under-estimated the drag coefficient while the results obtained using fine and very fine mesh were in agreement as shown in Table 3.2. The highly refined grid required greater computational effort and hence the medium grid was taken into consideration for further study.

	Number of Cells	Angle of Attack	$C_L Num$	$C_L Expt$	Percent Error	$C_D Num$	$C_D Expt$	Percent Error
1	27150	5°	0.283	0.24	17.9	0.103	0.128	19.5
2	108600	5°	0.2342	0.24	2.41	0.1279	0.128	0.07
3	434400	5°	0.2342	0.24	2.41	0.1279	0.128	0.07

Table 3.2: Comparison of numerical results with the experimental data at different refinement levels

Chapter 4

Effect of Solver Flow Type

4.1 Performance of Conventional Models

Numerical simulations were performed on a NACA0012 airfoil at at a Reynolds Number of 1000 and various angles of attack using the piso algorithm in Open-FOAM. Both the laminar and the one equation- SA model was used for performing the simulation and comparisons were made between the two. The experimental results of Liu. et. al was used for validation purpose. The lift and drag coefficient along with the percentage error between the numerical and experimental results have been shown in table 4.1

	Angle of Attack	$C_L Num$	$C_L Expt$	Percent Error	$C_D Num$	$C_D Expt$	Percent Error
				laminar			
1	0°	0	0	–	0.1199	0.12	0.08
2	5°	0.2342	0.24	2.41	0.1279	0.128	0.07
3	10°	0.339	0.421	19.4	0.15176	0.17	10.72
				Spalarat Allmaras			
1	0°	0	0	–	0.1182	0.12	1.5
2	5°	0.244	0.24	1.6	0.1286	0.128	0.4
3	10°	0.5457	0.421	29.6	0.2238	0.17	31.6

Table 4.1: Comparison of the laminar and SA model for a Reynolds Number of 1000

It was observed that the performance of the laminar and SA model was almost identical at 0 degree Angle of attack with the error in drag coefficient being slightly higher in case of SA model. As the angle of attack was increased, the ability of the
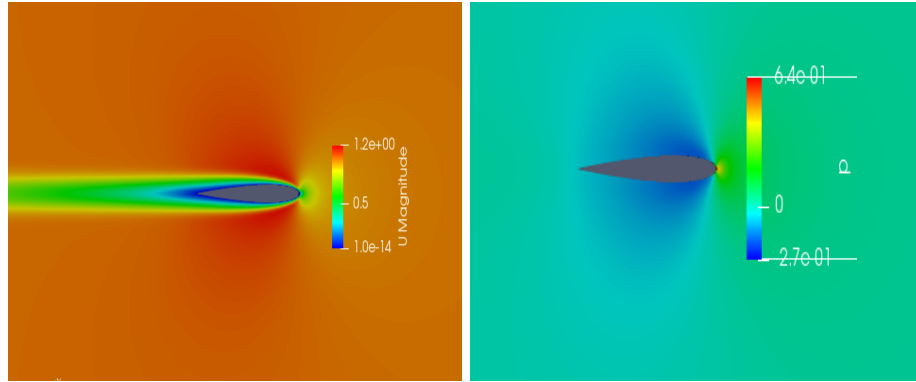
Figure 4.1: velocity and pressure contour obtained from laminar and SA model at an AoA of 0 degree
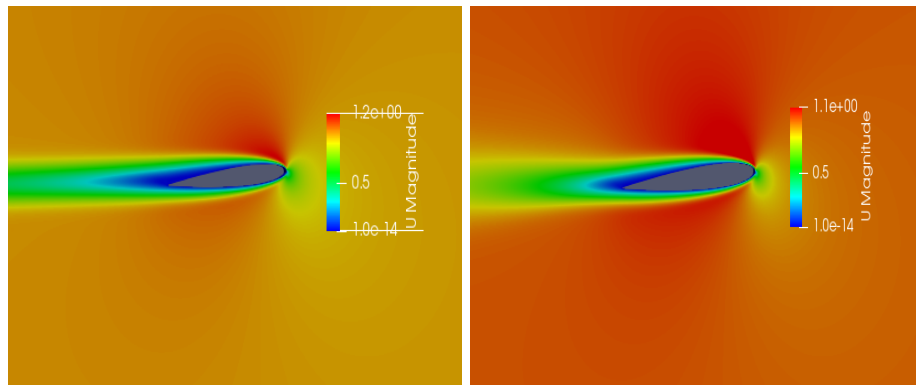
Figure 4.2: velocity contour obtained from (a)laminar and (b)SA model at an AoA of 5 degrees

laminar model to predict the lift and drag coefficient decreased and at an angle of attack of 10 degrees, it failed to predict the lift and drag coefficients. To the contrary, SA model showed a reduction in error as the angle of attack is increased. However, it too failed to predict the lift and drag coefficients at 10 degrees angle of attack. As mentioned earlier, at this flow condition, the fluid particle does not have enough energy to sustain the adverse pressure gradient, leading to flow separation. As the flow separates, transition from laminar to turbulent regime takes place and the fluid particle gains energy, thereby reattaching to the surface,forming a separation bubble. Thus the flow actually is neither fully laminar nor fully turbulent, but rather a blend of both with a transition region in between.

An important observation here is that the laminar model underpredicted the lift and the drag coefficient whereas the SA model overpredicted it. Thus if a model is introduced that can switch its behaviour from laminar to turbulence modeling
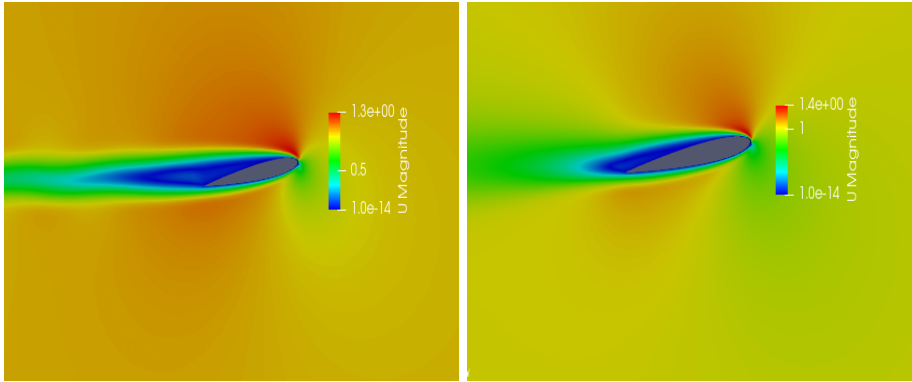
Figure 4.3: velocity contour obtained from (a)laminar and (b)SA model at an AoA of 10 degrees

through iterative process, the flow characteristics can be predicted.

Chapter 5

Conclusion and Future Work

In order to compare the model's ability to capture flow physics, the effect of domain proximity and mesh resolution was investigated. The results of experiments conducted by Liu et. al. on a NACA0012 airfoil at a Reynolds number of 1000 was utilized for validation purpose. Two computational domains extending having an extent of 10c and 15c beyond the trailing edge of the airfoil were taken into consideration. It was observed that effect of boundary proximity on the numerical results were less significant for a domain extension greater than or equal to 10c away from the trailing edge of the airfoil. This was followed by a grid independence test which rendered our model independent of mesh resolution. Once this was done, the model which was able to capture the flow physics with a lesser computational requirement was taken into further consideration. Using the optimum domain size and mesh resolution, numerical simulation was performed on a NACA0012 airfoil at a Reynolds Number of 1000 and at different angles of attack. The pressure and velocity contours were analyzed and the lift and drag coefficients were compared with the available data from Liu et. al.. Comparison was made between the laminar and the one-equation SA model. It was observed that the ability of laminar model to give accurate results decreased with an angle of attack while that of SA model increased. However both the models failed to give accurate results at an angle of attack of 10 degrees. It was observed that the laminar model underpredicted the lift as well as the drag coefficient whereas the SA model overpredicted them. The prime reason for this was the fluid particle not having enough energy to overcome the adverse pressure gradient, thus separating. This leads to transition from laminar to turbulent regime and thus the fluid particle gains energy and reattaches to the surface, forming a separation bubble which becomes difficult to capture using conventional models.

Appendix A

References

[1] Y. Liu, K. Li, J. Zhang, H. Wang, L. Liu, Numerical bifurcation analysis of static stall of airfoil and dynamic stall under unsteady perturbation

[2] Aerodynamics of an Airfoil at Ultra-Low Reynolds Number, Alam et. al

[3] Low Reynolds Number Airfoils, PBS Lissaman

[4] Low speed single element airfoil synthesis, McMasters, J.H. Henderson

[5] NACA Airfoils, NASA

[6] Openfoam user manual, www.openfoam.org

[7] CFD Online, www.cfdonline.com

[8] XFoil User Primer, Mark Drela, MIT Aero Astro Harold Youngren, Aerocraft, Inc.

[9] An engineering approach to the calculation of Aerodynamic Flows, Tuncer Cebeci

[10] Introduction to Fluid Mechanics, Robert W. Fox

[11] Turbulence Model Selection for Low Reynolds Number Flows, Aftab et.al.

[12] Calculations of flow around airfoils using two Dimensional RANS, Aleksey A. Matyushenko, Elsevier

[13] Aerodynamic Characteristics of Seven Symmetrical Airfoil Sections Through 180-Degree Angle of Attack for Use in Aerodynamic Analysis of Vertical Axis Wind Turbines, Robert E. Sheldahl

[14] Drag Prediction in Transitional Flow over Airfoils, Wassim A. Basha,JOURNAL OF AIRCRAFT

[15] Fluid flow around NACA 0012 airfoil at low-Reynolds numbers with hybrid lattice Boltzmann method, Elio et. al.

[16] https://www.simscale.com/forum/t/what-is-y-yplus/82394